Closely-packed UWB MIMO/diversity antenna with different patterns and polarizations for USB dongle applications

Zhang, Shuai; Lau, Buon Kiong; Sunesson, Anders; He, Sailing

Published in:
IEEE Transactions on Antennas and Propagation

DOI:
10.1109/TAP.2012.2207049

2012

Document Version:
Peer reviewed version (aka post-print)

Closely-Packed UWB MIMO/Diversity Antenna with Different Patterns and Polarizations for USB Dongle Applications

Shuai Zhang, Buon Kiong Lau, *Senior Member, IEEE,* Anders Sunesson and Sailing He, *Senior Member, IEEE*

***Abstract*—A closely-packed ultrawideband (UWB) multiple-input multiple-output (MIMO)/diversity antenna (of two elements) with a size of 25 mm by 40 mm is proposed for USB dongle applications. Wideband isolation can be achieved through the different patterns and polarizations of the two antenna elements. Moreover, the slot that is formed between the monopole and the ground plane of the half slot antenna is conveniently used to further enhance the isolation at the lower frequencies and to provide an additional resonance at one antenna element in order to increase its bandwidth. The underlying mechanisms of the antenna's wide impedance bandwidth and low mutual coupling are analyzed in detail. Based on the measurement results, the proposed antenna can cover the lower UWB band of 3.1-5.15 GHz, and within the required band, the isolation exceeds 26 dB. The gains and total efficiencies of the two antenna elements are also measured. Furthermore, a chassis mode can be excited when a physical connection is required between the ground planes of the two antenna elements. Without affecting the performance of the half slot element, the monopole can now cover the band of 1.78-3 GHz, apart from the UWB band. The proposed antenna structure is found to provide good MIMO/diversity performance, with very low envelope correlation of less than 0.1 across the UWB band.**

***Index Terms*—MIMO, UWB antenna, pattern diversity, polarization diversity, mutual coupling**

I. Introduction

ULTRAWIDEBAND (UWB) systems have been drawing considerable interests because of their very high data rates and low operating power level. Moreover, the low power feature enables frequency reuse, since it does not cause significant interference in nearby devices. Since then, there have been many papers on designing high performance and cost effective single-element UWB antennas (see e.g., [1]-[3]). In order to further increase data throughput and/or combat multipath fading, the multiple-input multiple-output (MIMO) /diversity technology has been considered for UWB systems [4]-[5]. Both MIMO and diversity antennas require low mutual coupling among the antenna elements in the operating bands. However, because of the limited space in USB dongles and other small terminals, the mutual coupling between the UWB antenna elements can be very large. Furthermore, it is far more difficult to maintain a low level of mutual coupling within an ultrawide band than a narrow band. Therefore, it is a challenging topic to design UWB MIMO/diversity antennas with extremely compact structures and high isolation over an ultrawide band.

A number of studies have been carried out to reduce the size of UWB MIMO/diversity antennas and/or enhance the wide band isolation [6]-[13]. In [6]-[8], various decoupling structures have been inserted between two UWB antenna elements, and different polarizations have been utilized in [9]-[11]. In those designs, mutual coupling can be reduced over the large design bandwidths. However, the sizes of the UWB diversity antennas in [6]-[11] are too large for USB dongle applications. A more compact UWB MIMO/diversity antenna is proposed in [12], and it can cover the entire UWB band of 3.1-10.6 GHz with an isolation of over 16 dB. However, a complicated tree-like structure, which functions as a wideband parasitic scatterer [13], has to be designed between the antenna elements to reduce coupling. Moreover, due to the problem of severe dispersion, the full UWB band has recently been separated into the lower UWB band (3.1-5.15 GHz) and the higher UWB band (5.875-10.6 GHz), with the lower band being far more commonly used. Consequently, the design requirement has been relaxed to a certain degree. In [14], a compact printed UWB diversity antenna system with the size of 37 mm × 45 mm = 1665 mm^2 has been proposed for USB dongle applications. It can cover the lower UWB band of 3.1-5 GHz and has an isolation of higher than 20 dB. The high isolation is achieved through a combination of polarization diversity and ground plane current mitigation. To further miniaturize MIMO/ diversity antennas for USB dongles, it is more important to decrease the antenna width than its length. However, this is hard to achieve with existing design techniques, e.g., [6]-[14].

In this paper, a closely-packed UWB MIMO/diversity antenna is proposed for USB dongle applications. The mutual

The work was supported in part by VINNOVA under Grant no. 2008-00970 and VR under Grant no. 2010-468 and also in part by a scholarship within EU Erasmus Mundus External Cooperation Window TANDEM.

S. Zhang and S. He are with the Division of Electromagnetic Engineering, School of Electrical Engineering, Royal Institute of Technology, S-100 44 Stockholm, Sweden and also with the Centre for Optical and Electromagnetic Research, Zhejiang University, Hangzhou 310058, China (e-mail: sailing@ieee.org).

B. K. Lau and A. Sunesson are with the Department of Electrical and Information Technology, Lund University, SE-221 00 Lund, Sweden.

A. Sunesson was with Lite-On Mobile AB, SE-223 63 Lund, Sweden. He is now with European Spallation Source ESS AB, SE-22100 Lund, Sweden.

coupling is mainly reduced by the distinct radiation patterns and polarizations of the two antenna elements. Moreover, instead of suffering from effects of close proximity, the antenna takes advantage of a semi-circular slot formed by the edges of its two closely spaced elements to further enhance the isolation at the lower frequencies, as well as to excite an additional resonance for one element to increase its bandwidth. From the measured results, it can cover the lower UWB band of 3.1-5.15GHz and the measured isolation exceeds 26 dB within the required band. The size of the proposed antenna is 25 mm × 40 mm = 1000 mm^2, which is 40% smaller than that of [14], while similar performance is achieved by both antennas. Furthermore, the width of the proposed MIMO antenna has been effectively reduced from 37 mm to 25 mm (relative to the antenna in [14]), making it more suitable for USB dongle applications.

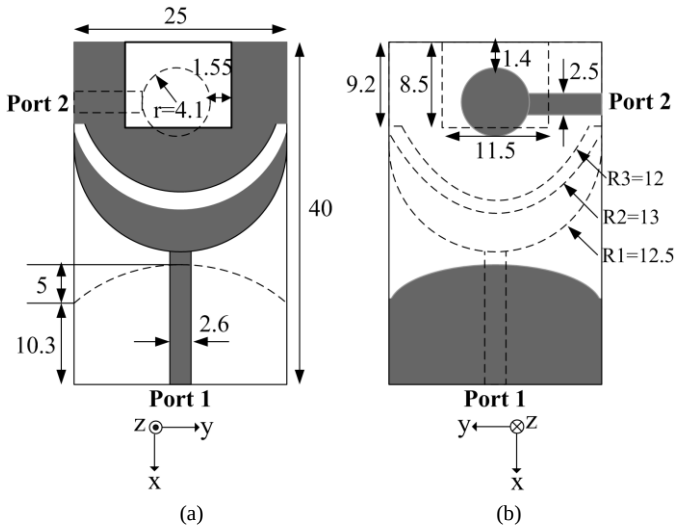

Fig. 1. Detailed geometry of the proposed UWB MIMO/diversity antenna: (a) top view, (b) back view. The grey area represents the copper layer and the dashed lines trace the edges of the copper layer on the opposite side of the PCB.

II. Antenna Configuration, Underlying Mechanisms and Feeding Considerations

A. Antenna Configuration

The geometry of our proposed UWB MIMO/diversity antenna is shown in Fig. 1. The two UWB antenna elements are printed on a 25 mm × 40 mm FR4 PCB substrate, which has a thickness of 1.55 mm, a dielectric permittivity of 4.7 and a loss tangent of 0.015. Antenna 1 is a traditional (UWB) monopole antenna that has been modified into a crescent shape in order to increase the length of the slot formed by the crescent shaped monopole and the ground plane of Antenna 2. This semi-circular slot can enlarge the bandwidth of Antenna 2 and increase the isolation between Antennas 1 and 2 at the lower frequencies, which will be analyzed in the next section. The centers of the incomplete circles indicated by R1, R2 and R3 are 28.5 mm, 33.8 mm and 34.8 mm away (along the negative *x*-axis) from the midpoint along the bottom edge of the PCB, respectively. The radiuses of these circles are given in Fig. 1 as 12.5 mm, 13 mm and 12 mm, respectively. Additionally, in order to improve impedance matching, the ground plane of Antenna 1 has been changed into a semi elliptical shape with a minor axis of 5 mm and a prolate axis of 40 mm. Antenna 2 is a half UWB slot antenna which is modified from the full UWB slot antenna in [15]. This kind of half slot antenna has the advantage of small size, wide bandwidth and good directional property. The monopole and half slot antenna elements form a complementary antenna pair, which helps to reduce the mutual coupling between the two elements. The detailed parameters of the proposed antenna are provided in Fig. 1.

B. Underlying Bandwidth and Isolation Mechanisms

In Fig. 2, the simulated S parameters of the designed UWB MIMO/diversity antenna are presented. The simulation results are obtained using the time-domain solver of CST Microwave Studio. For the simulation, discrete ports are utilized for the two antenna elements, since the results they produce better reflect the measured results than those achieved using waveguide ports. It can be observed in Fig. 2 that a wide band isolation of over 23 dB can be achieved within the required band (3.1-5.15 GHz). In practice, the two antennas can be fed with a thin cable (50 ohm) as shown in Fig. 3. Fig. 4 shows the simulated results with this cable fed structure, which are very similar to those in Fig. 2.

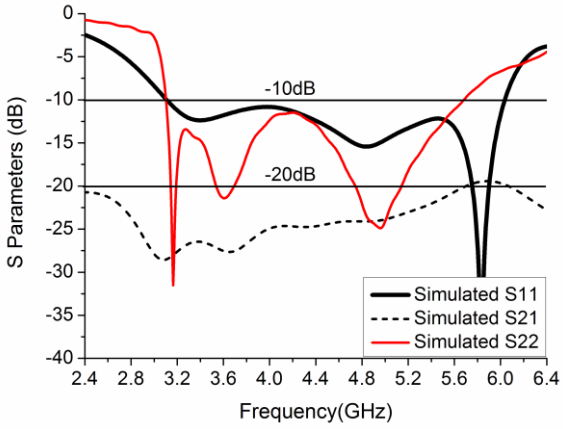

Fig. 2. Simulated S parameters of the proposed UWB MIMO/diversity antenna.

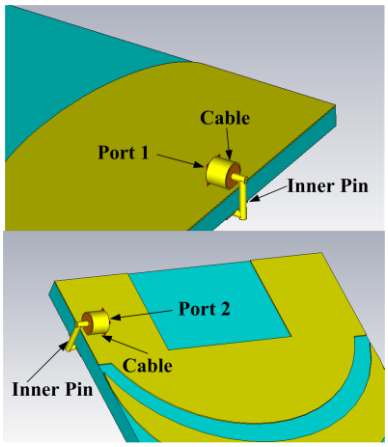

Fig. 3. UWB MIMO antenna fed by two thin cables.

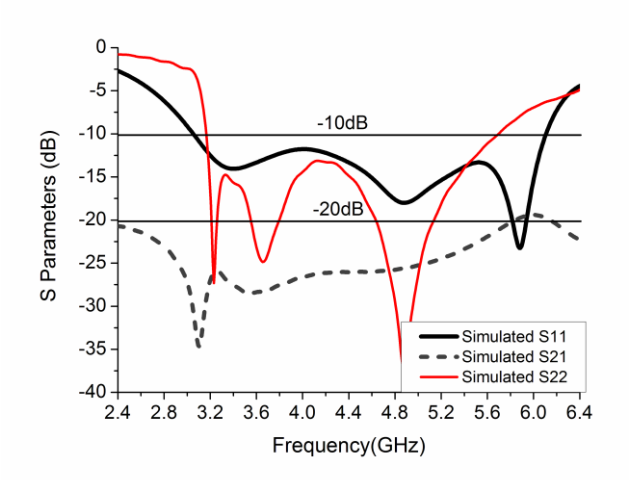

Fig. 4. S parameters for the UWB MIMO antenna fed by two thin cables.

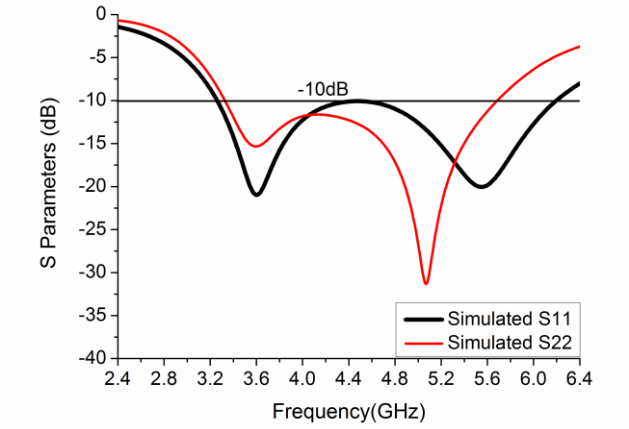

Fig. 5. Simulated S parameters with only the monopole antenna element (port 1) or only the half slot antenna element (port 2).

To gain more insight into the impedance bandwidth of the proposed antenna, we illustrate in Fig. 5 the simulated S parameters for only the monopole antenna (port 1/Antenna 1) or only the half slot antenna (port 2/Antenna 2). It can be observed that the monopole antenna has a wider 10 dB impedance bandwidth and a lower band edge than the half slot antenna, with the half slot antenna having two resonances at around 3.6 GHz and 5.1 GHz (see Fig. 5). But when the two antenna elements are put close to each other in a co-planar manner, the lower resonant frequency of the monopole antenna decreases more than that of the half slot antenna. This is because capacitance that results from the proximity of the monopole and the ground plane of the half slot directly increases the electrical length of the monopole antenna (i.e., as capacitive top loading), whereas for the half slot antenna, the capacitance is only introduced to its ground plane. In order to enlarge the bandwidth of the half slot antenna at the lower band edge, a third resonance is excited at 3.2 GHz by optimizing the slot formed by the monopole antenna and the ground plane of the half slot antenna. In particular, the formed slot has been modified into a crescent shape, such that the increased slot length supports the relatively low resonant frequency of 3.2 GHz for the half slot antenna. In this way, the two antenna elements can both cover the lower UWB band of 3.1-5.15 GHz. In addition, a third resonance is excited at about 5.8 GHz for the monopole antenna, due to its higher order mode.

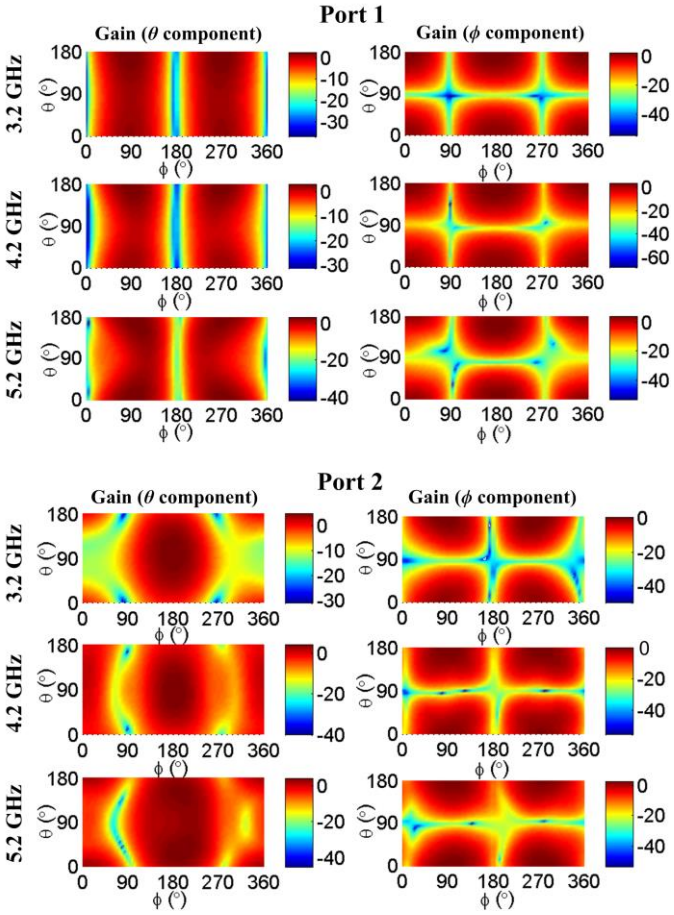

Fig. 6. Simulated radiation patterns of Antennas 1 and 2 at 3.2 GHz, 4.2 GHz, and 5.2 GHz.

For both diversity and MIMO applications, it is crucial for the two antenna elements to offer low mutual coupling. In the proposed MIMO/diversity antenna, three physical mechanisms work together to facilitate the high isolation between the two antenna elements:

1) *Angle diversity* – Antenna 1 is a traditional (UWB) monopole antenna whose radiation pattern (regardless of the frequency) always has a null pointing in the direction of negative *x*-axis. On the other hand, Antenna 2 is a semi UWB slot antenna that is directional and its main beam is pointing in the direction of negative *x*-axis. Hence, the two antennas can realize angle diversity in their radiation patterns. This mechanism mainly works from 3.4 GHz to 5.15 GHz. Fig. 6 shows the simulated 3D radiation patterns for Antennas 1 and 2 at 3.2 GHz, 4.2 GHz, and 5.2 GHz. The ϕ and θ angles are the azimuth and elevation angles in the polar coordinates, which are respectively angles from the +ve x-axis in the anticlockwise direction and angles from the +ve z-axis in Fig. 1(a). The ϕ and θ polarization components are similarly defined. The angle diversity can be clearly observed by comparing the patterns of co-polarized components between the two ports.

2) *Decoupling slot formed by the monopole antenna and the ground plane of the half slot antenna* – This slot not only provides a resonance for Antenna 2 at 3.2 GHz, but it also operates as a decoupling structure at around 3 GHz (see the null of S_{21} in Fig. 4). This mechanism enhances the isolation from 3.1 to 3.4 GHz. The idea of naturally formed decoupling slot has been studied in the context of decoupling closely spaced narrowband PIFAs [16]. It can also be interpreted as a compact implementation of the parasitic scatterer technique [13], which introduces a resonant structure in between closely spaced antennas to achieve decoupling. In order to do a parametric study of the slot shapes, a stub slot of length l is added (see Fig. 7). The results from the parametric study of the slot shape are illustrated in Fig. 8. As the length l increases, the nulls in S_{22} and S_{21} at 3.2 GHz and 3.1 GHz, respectively, monotonically decrease in frequency. Moreover, the current distribution of Antenna 2 at 3.2 GHz is given in Fig. 9. It can be observed that the coupling currents are concentrated along the edges of the slot.

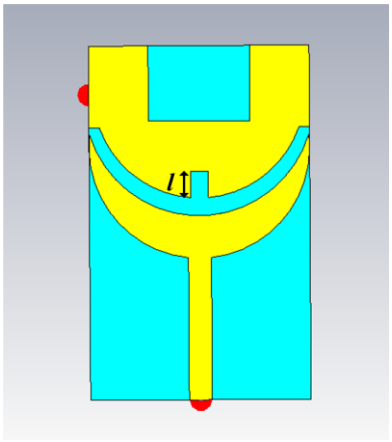

Fig. 7.The stub slot of length *l* for the parametric study of the slot shape.

In addition, besides increasing the slot length, modifying the formed slot into a crescent shape also helps to direct the main lobe of the half slot antenna's radiation pattern towards the negative *x*-axis, without changing the radiation pattern of the monopole. The radiation patterns with and without the presence of the other element are shown in Fig. 6 and Fig. 10, respectively, at 3.2 GHz. For Antenna 1, the patterns (with and without the other element) do not differ significantly. But for Antenna 2, the pattern in Fig. 6 (with the other element) is more directional than that in Fig. 10 (without the other element). In this way, the radiation patterns of the two antennas elements become effectively orthogonal in the 3.1 to 3.4 GHz band.

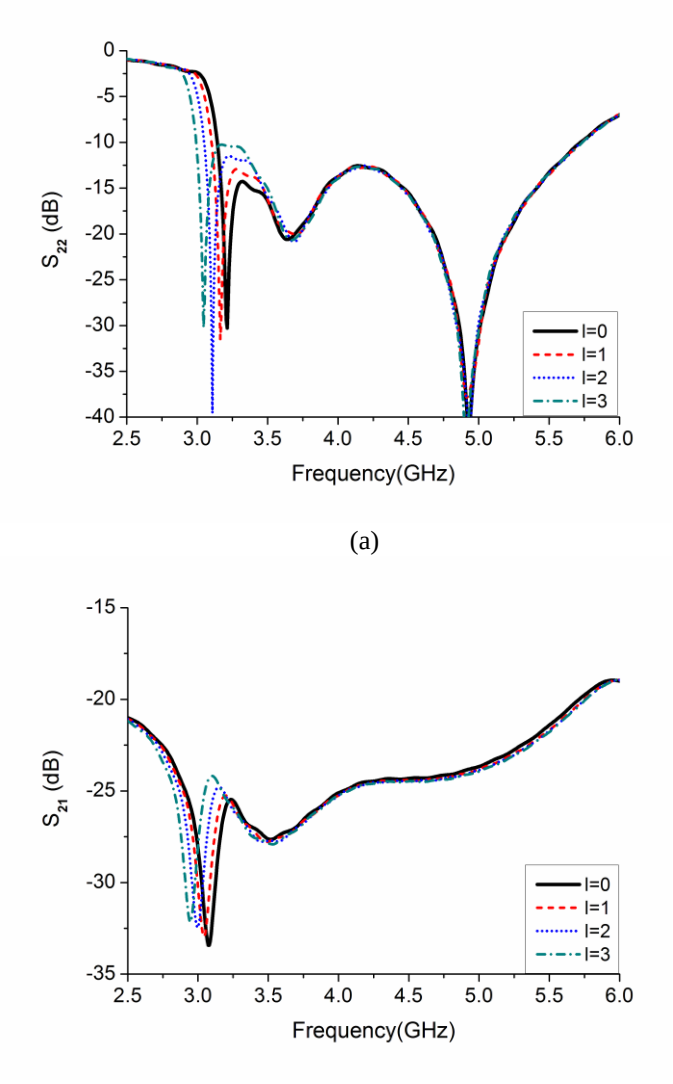

Fig. 8. (a) S_{22} and (b) S_{21} with different lengths of the stub slot *l*.

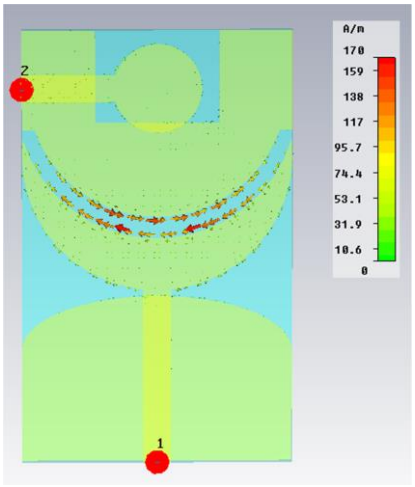

Fig. 9. The current distributions of Antenna 2 at 3.2 GHz.

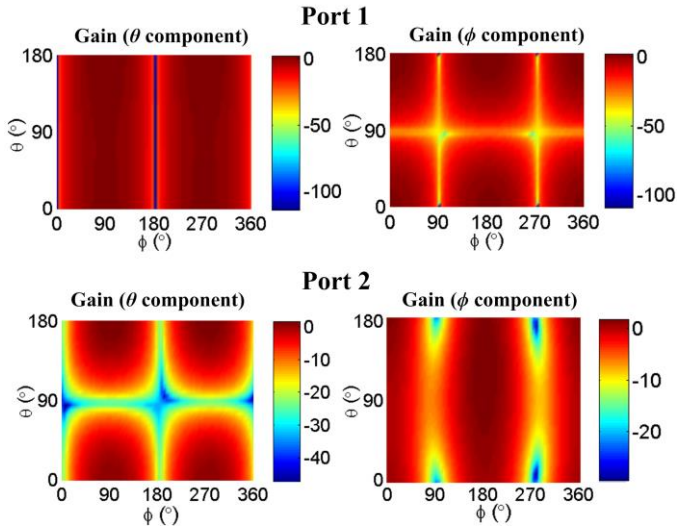

Fig. 10. Simulated radiation patterns at 3.2 GHz when only the monopole antenna (Port 1) is present and when only the semi UWB slot antenna (Port 2) is present.

3) *Polarization diversity* – This mechanism works for the entire lower UWB band (3.1-5.15 GHz). In particular, Antenna 1 (monopole) is primarily polarized in the *x* direction, whereas Antenna 2 (half slot) is mainly polarized along the *y* direction. Table 1 shows the simulated power level difference in the patterns of the two polarization components (θ component (dB) minus ϕ component (dB)) in the *x*-*z* and *y*-*z* planes. It can be observed that: for the monopole antenna element, the purity of polarization can be kept in a very good level (above 19.2 dB) for the two planes. For the half slot antenna element, the purity of polarization in the *x*-*z* plane is quite high but has decreased to 4.7-7.3 dB in the *y*-*z* plane. This is because the shape of the half slot is very wide, which increases the power level along the *x* direction. However, because of the first two decoupling mechanisms, the radiation patterns of two antenna elements have been separated and the overlapped parts of gain patterns mainly focus around the *x*-*z* plane. Therefore, although the polarization purity of Antenna 2 on the *y*-*z* plane is inadequate, angle and polarization diversities complement each other to ensure high isolation between the two elements. Fig. 11 shows the simulated and measured θ *and* ϕ components for Antennas 1 and 2 in the *x*-*z* plane. As can be observed, the polarizations for two elements are quite orthogonal to each other.

TABLE I
POWER LEVEL DIFFERENCE (θ COMPONENT PEAK VALUE (IN dB) MINUS ϕ COMPONENT PEAK VALUE (IN dB) IN THE SELECTED PLANE)

Frequency (GHz)	*x*-*z* plane		*y*-*z* plane	
	Monopole	Half Slot	Monopole	Half Slot
3.1	24.8 dB	-26.1 dB	-28.9 dB	4.7 dB
3.5	25.2 dB	-22.4 dB	-23.9 dB	6 dB
4	25.1 dB	-20.5 dB	-24.8 dB	5.2 dB
4.5	23.7 dB	-18.5 dB	-24.4 dB	7.3 dB
5.2	21.2 dB	-12.8 dB	-19.2 dB	6.9 dB

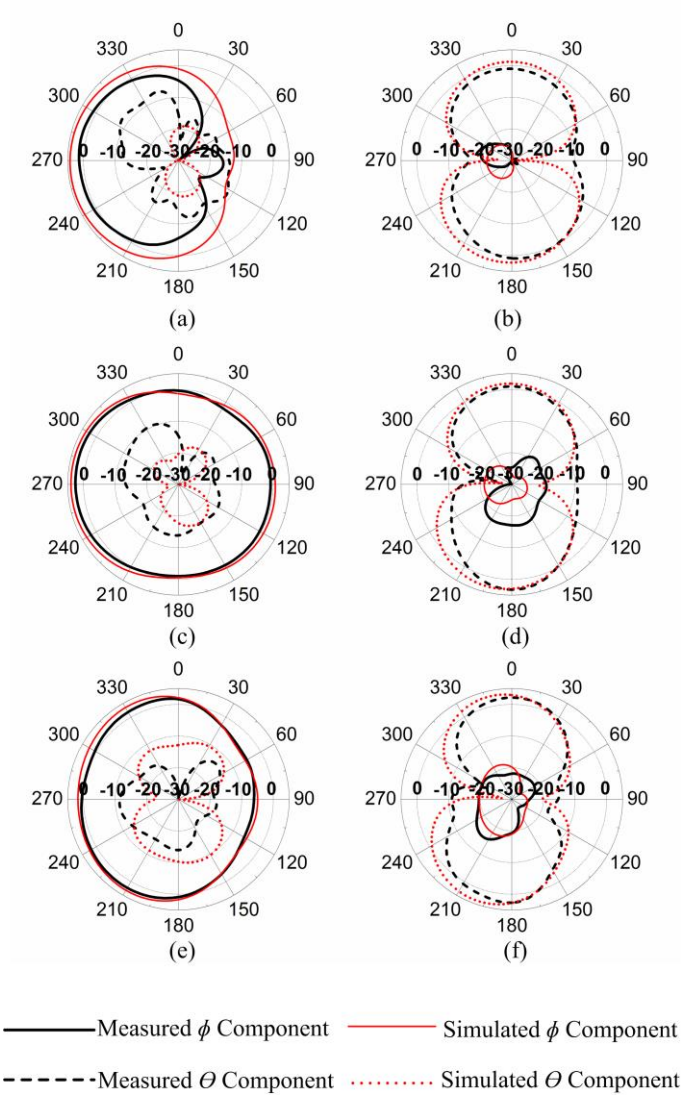

Fig. 11. The comparison between the simulated and measured θ and ϕ components in the *x*-*z* plane for Antenna 1 at (b) 3.2 GHz, (d) 4.2 GHz, (f) 5.2 GHz and Antenna 2 at (a) 3.2 GHz, (c) 4.2 GHz, (e) 5.2 GHz

Based on the mechanisms described above, good impedance bandwidth and isolation can be achieved over a wide band, despite the two elements being placed very close to each other (i.e., the distance between the two elements is about 1 mm).

C. Practical Antenna Feeding Considerations

In practical implementation, if the USB connectors are located at the +ve x side (see Fig. 1), a long feed cable is needed to excite port 2. If the ground planes of the two antennas do not need to be connected, then the cable can be attached to the inner surface of the USB dongle casing. As an example, the cable can be 5 mm above the ground plane of Antenna 2. In this way, the performance of two antennas is similar as before.

On the other hand, it is also possible that the two antennas need to share a common ground. Fig. 12 shows one possible configuration of Antennas 1 and 2 with connected ground planes. In order to physically connect the ground planes of the two antennas, the ground planes have been moved to the same

side of the PCB. A thin cable-like structure is soldered on points A and B (see Fig. 12) of the ground planes to mimic part of the feed cable for Antenna 2. From our studies, if soldered points A and B move along the central line of the whole antenna structure, the performances of two antennas are almost unchanged. However, the performances are sensitive to the distance between the thin cable and the PCB substrate. In order to solve this problem, a small FR4 PCB block with the thickness of 1.55 mm is used to keep the cable-substrate distance unchanged. This is because the thin cable is placed on the small block. For this feed arrangement, only two parameters of the UWB MIMO antenna are slightly different from those given in Fig. 1. In particular, the ground plane length of the monopole antenna and the centers of the incomplete circles R3 have been modified from 10.3 mm and 34.8 mm to 12 mm and 33.8 mm, respectively.

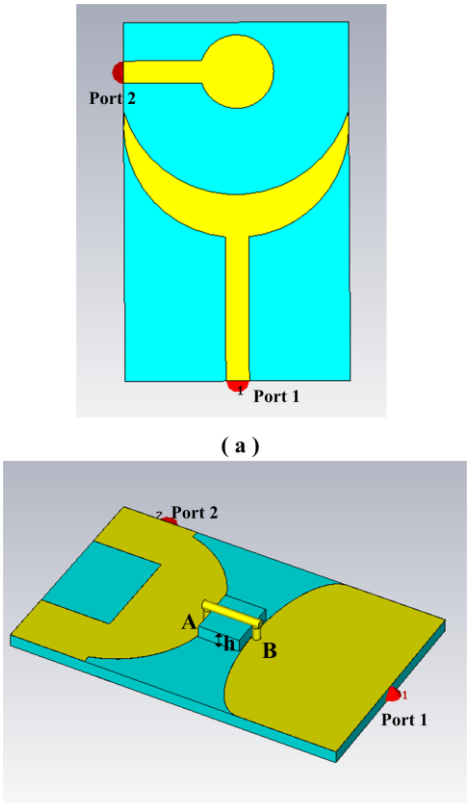

Fig. 12. The connected ground planes of Antennas 1 and 2 (through the feed cable for Antenna 2) in one possible practical implementation.

The S parameters of UWB MIMO antenna with the connected ground plane are shown in Fig. 13. For the UWB MIMO band the two antennas can still cover the band of 3.1-5.15 GHz with an isolation of over 25 dB. The performance of Antenna 2 remains largely the same. However, a dipole-like chassis mode is excited in Antenna 1 due to the connection of the ground plane, which results in the first resonance being moved to the 1.9 GHz band. Through proper optimization with the -6 dB specification, the monopole can now cover the additional band of 1.78-3 GHz, which can be utilized for a wide range of services including UMTS 3G (1.8-2.2 GHz), WiMAX (2.3-2.4 and 2.5-2.7 GHz), WLAN (2.4-2.5 GHz) and LTE (2.5-2.7 GHz). Furthermore, the simulated efficiency for the monopole antenna from 1.78-3 GHz is found to be above 60%. Nevertheless, if these wireless services are not needed, then the additional pass-band of 1.78-3 GHz may introduce some adjacent band interference in the signal.

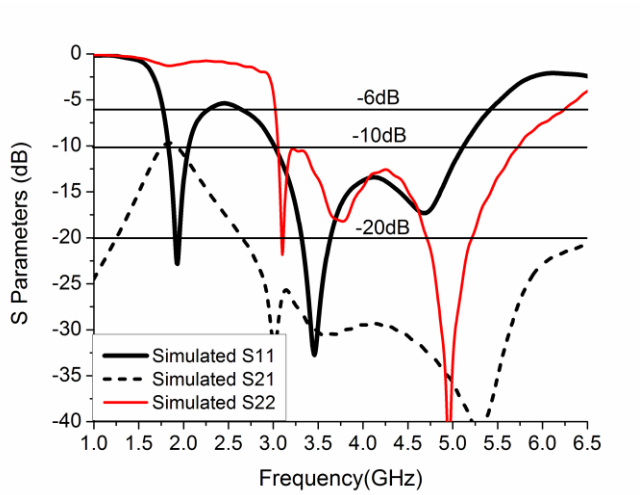

Fig. 13.S parameters for the UWB MIMO antenna with the connected ground planes of Antennas 1 and 2 through the feed cable for Antenna 2.

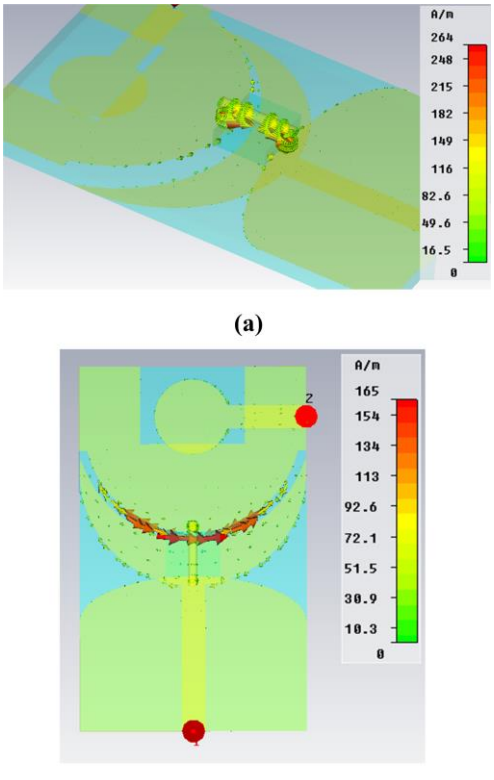

Fig. 14. Current distributions for the UWB MIMO antenna with the connected ground planes of Antennas 1 and 2 at (a) 1.9 GHz and (b) 3 GHz.

In order to further clarify the underlying mechanisms of the MIMO UWB antenna with the connected ground, the current distributions at 1.9 and 3.1 GHz are provided in Fig. 14. In Fig.

14(a), the currents mainly focus on the connecting thin cable due to the dipole-like chassis mode (current is strongest in the middle of the whole ground plane). For Fig. 14 (b), the currents are still concentrated around the slot, which is similar to the case without the connecting ground plane in Fig. 9. Through the S parameters and current distribution, we find that the formed slot still works well in providing decoupling as well as an additional resonance.

III. Measurement Results and MIMO Performance

In this section, the performance of our proposed UWB MIMO/diversity antenna is verified through measurement and some discussions are provided. The prototype of the proposed compact antenna is shown in Fig. 15, together with a €1 coin.

Fig. 15. Prototype of the proposed UWB MIMO/diversity antenna.

A. S-Parameters

The measured S parameters of the designed antenna are presented in Fig. 16. The measured impedance bandwidths of the two antennas are from 3.13 GHz to 6.2 GHz, where the lowest operating frequencies are a little higher than the simulations due to permittivity variation of between 4.0 and 4.9 in the FR4 substrate. In practice, in order to verify permittivity variation one can construct a 50 ohm microstrip line of known physical length using the same FR4 substrate, and measure the phase delay. This can be used to calibrate the permittivity of the FR4. Here, the permittivity of the FR4 substrate is determined to be around 4.5, which is a little lower than the simulation value of 4.7. Nevertheless, the proposed UWB MIMO/diversity antenna can still approximately cover the lower UWB band of 3.1-5.15 GHz. Within the required band, the isolation is over 26 dB.

During all the measurements (including S parameters, radiation patterns, gains and efficiencies), in order to mitigate currents flowing from the ground plane onto the feed cables, two ferrites (see the black rings in Fig. 17) are utilized. The measured S parameter results in Fig. 16 agree quite well with the corresponding simulated results in Figs. 2 and 4. For example, the three resonances observed in the simulated results are also present in the measured results.

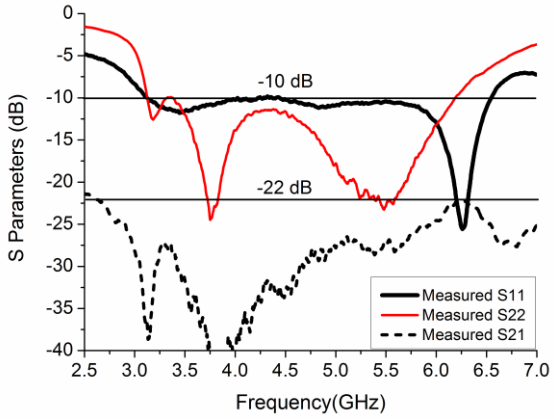

Fig. 16. Measured S parameters of the proposed UWB MIMO/diversity antenna.

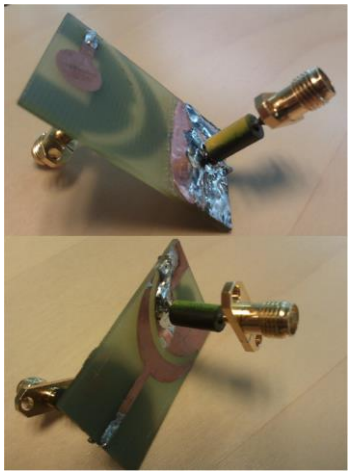

Fig. 17. The ferrite rings on the feed cables.

B. Radiation Patterns

The 3D radiation patterns of our proposed UWB MIMO/diversity antennas are measured in an anechoic chamber and shown in Fig. 18. When one antenna is measured, the other is terminated with a 50Ω load. It can be observed that the radiation patterns of two antenna elements can complement with each other very well and the measured results are similar to the simulated ones in Fig. 6. The similarities between the measured and simulated results can also be seen in Fig. 11 for the *x*-*z* plane. In addition, the measured polarization property is illustrated in Fig. 11. In the *x*-*z* plane, Antenna 2 points towards the direction of 270°, with a strong ϕ component, whereas for Antenna 1, there is null at 270°, with a strong θ component. Thus, polarization diversity can be achieved effectively. Such characteristics contribute to the high isolation achieved by the proposed compact MIMO/diversity antenna.

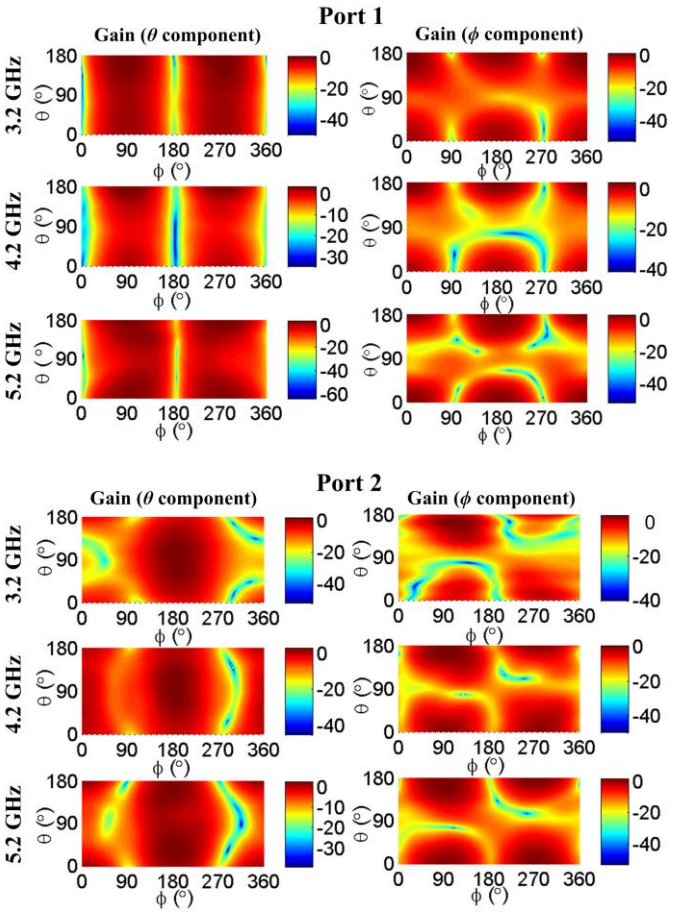

Fig. 18. Measured 3D radiation patterns for Antennas 1 and 2 at 3.2 GHz, 4.2 GHz, and 5.2 GHz.

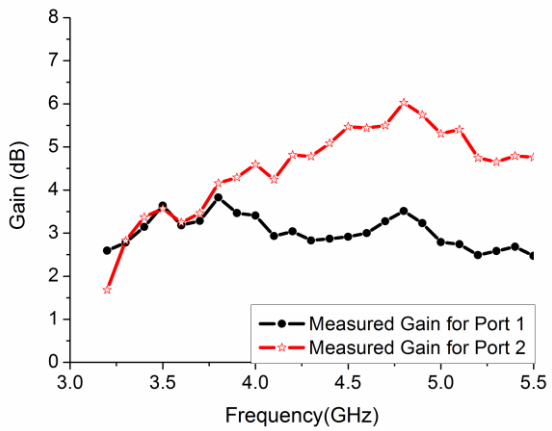

Fig. 19. Measured peak gains for Antennas 1 and 2.

C. Gain and Total Efficiency

Gains and total efficiencies of Antennas 1 and 2 are also measured and obtained through their 3D radiation patterns. In order to eliminate the little effects of mismatching at 3.1GHz the gains and total efficiencies starts from 3.2 GHz. Figure 19 shows the measured the gains of two antenna elements within the lower UWB band are larger than 1.5 dB. In Fig. 20 the total efficiencies of Antennas 1 and 2 are presented. Due to the introduction of two ferrite rings in Fig. 17, all the measured results are very similar to those from simulations. The only disadvantage is that the ferrites reduce the total efficiency by around 25%, due to the suppression of leakage ground currents. However, it can be observed in Fig. 20 that the two antenna elements are still quite efficient. It is also noted that the ferrites are not used in practice and therefore the efficiency values can be much higher than those shown in Fig. 20.

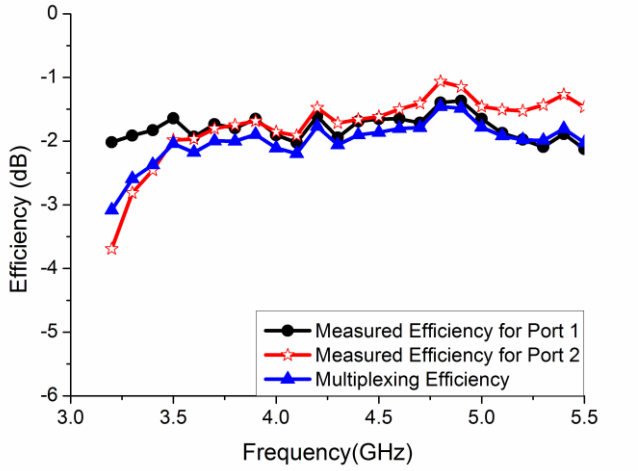

Fig. 20. Multiplexing efficiency and measured total efficiencies for Antennas 1 and 2.

D. Correlation, Diversity Gain and Multiplexing Efficiency

The envelope correlation coefficient ρ_e between the two elements can be calculated using the measured 3D radiation pattern as well as the assumed angular power spectrum (APS) of the incoming waves [17]. Assuming uniform 3D APS, the envelope correlation is found to be lower than 0.1 over the entire operating band.

For the diversity gain, a good diversity performance can be achieved as long as the correlation coefficient is less than 0.7 and two antenna elements have a similar mean effective gain (MEG) [17]. Moreover, under uniform 3D APS, the MEG of antenna i is simplified into $MEG_i = \eta_i/2$, where η_i is the total efficiency of the i-th antenna element. Since the two elements in the proposed antenna array have the similar efficiencies (see Fig. 20) and low envelope correlation, the requirements for good diversity performance are satisfied.

Furthermore, the capacity of a 2 × 2 MIMO channel with ideal transmit antennas (of zero correlation and 100% total efficiency) and the proposed MIMO UWB antenna at the receiver can be calculated using the measured correlation and efficiency performance [18]. However, here we focus on the multiplexing efficiency metric η_{MUX}, which is derived from capacity but conceptually simpler. η_{MUX} defines the difference in power required for a MIMO antenna-under-test (AUT) to obtain a given capacity relative to an ideal reference MIMO antenna of zero correlation and 100% total efficiency. It can be interpreted as generalized total efficiency, which not only account for the total antenna efficiency, but also correlation and

efficiency imbalance. Assuming uniform 3D APS, η_{MUX} is a closed form expression given by

$$\eta_{MUX} = \sqrt{(1-|\rho_c|^2)\eta_1\eta_2}\,, \qquad (1)$$

where ρ_c is the complex correlation coefficient between the two elements, and $\rho_e \approx |\rho_c|^2$. Fig. 20 shows the multiplexing efficiency calculated from our measured efficiency and envelope correlation coefficient. Since $\rho_e < 0.1$ in the band of interest, and the total efficiencies of the two antennas are similar, the multiplexing efficiency performance is similar to that of the measured total efficiency in Fig. 20. This indicates that the performance of the MIMO UWB antenna is mainly limited by the total efficiencies of the elements.

Besides the ferrite rings, bazooka/coax baluns are also very good choices for mitigating cable influence in antenna measurement. However, the fractional bandwidth of traditional bazooka/coax baluns is typically less than 10%. In some situations, when the current at the lowest frequency of the antenna's operating band is chocked, the currents at higher frequencies also become less sensitive to the cable. Nevertheless, in general, several bazooka/coax baluns operating at different frequencies are required for a wideband measurement. Therefore, in order to make the measurement accurate and simple, in the present paper we used ferrite rings which have very wide bandwidth (though some losses are introduced).

IV. Conclusion

In this paper, a closely-packed UWB MIMO/diversity antenna with a size of 25 mm × 40 mm is proposed for USB dongle applications. Through different radiation patterns and polarizations of the two antenna elements, wideband isolation has been achieved. The proposed antenna can cover the lower UWB band of 3.1-5.12 GHz with an isolation of higher than 26 dB. The underlying mechanisms that contribute to the good impedance bandwidth and high isolation are carefully explained. The radiation patterns, gains and efficiencies of two antenna elements have also been measured. The measurement results confirm that the proposed UWB MIMO/diversity antenna is suitable for MIMO USB dongle applications.

References

[1] J. Liang, C. C. Chiao, X. Chen and C. G. Parini, "Printed circular disc monopole antenna for ultra-wideband applications," *Electron. Lett.*, vol. 40, no. 20, pp.1246-1247, Sep.2004.

[2] M. J. Ammann and Z. N. Chen, "A wide-band shorted planar monopole with bevel," *IEEE Trans. Antennas Propag.*, vol. 51, no. 4, pp. 901–903, Apr. 2003.

[3] S. Zhang, S. N. Khan, and S. He, "Modified rhombic monopole antenna for low loss frequency notched UWB applications," *J. Electromagn.. Waves Appl.*, vol. 23, no. 2-3, pp. 361-368, 2009.

[4] V. Tran and A. Sibille, "Spatial multiplexing in UWB MIMO communications," *Electron. Lett.*, vol. 42, no. 16, pp. 931–932, 2006.

[5] L. Yang and G. B. Giannakis, "Analog space-time coding for multiantenna ultra-wideband transmissions," *IEEE Trans. Commun.*, vol. 52, no. 3, pp. 507–517, Mar. 2004.

[6] K. L. Wong, S. W. Su, and Y. L. Kuo, "A printed ultra-wideband diversity monopole antenna," *Microw Opt Technol Lett.*, vol. 38, no. 4, pp. 257–259, 2003.

[7] L. Liu, H. P. Zhao, T. S. P. See, and Z. N. Chen, "A printed ultrawideband diversity antenna," in *Proc. Int. Conf. Ultra-Wideband (ICUWB'2006)*, Waltham, MA, Sep. 24-27, 2006, pp. 351–356.

[8] S. Hong, K. Chung, J. Lee, S. Jung, S. S. Lee, and J. Choi, "Design of a diversity antenna with stubs for UWB applications," *Microw. Opt. Technol. Lett.*, vol. 50, no. 5, pp. 1352–1356, 2008.

[9] E. Antonino-Daviu, M. Gallo, B. Bernardo-Clemente and M. Ferrando-Bataller, "Ultra-wideband slot ring antenna for diversity applications," *Electron. Lett.*, vol. 46, no. 7, pp. 478-480, 2010.

[10] S. Zhang, P. Zetterberg, and S. He, "Printed MIMO antenna system of four closely-spaced elements with large bandwidth and high isolation," *Electron. Lett.*, vol. 46, no. 15, pp. 1052-1053, 2010

[11] Y. Lu and Y. Lin, "A compact dual-polarized UWB antenna with high port isolation," in *Proc. IEEE Int. Symp. Antennas Propagation Society International Symposium (APS'2010),* Toronto, Canada, Jul. 11-17, 2010.

[12] S. Zhang, Z. Ying, J. Xiong and S. He, "Ultrawideband MIMO/diversity antennas with a tree-like structure to enhance wideband isolation," *IEEE Antennas Wireless Propag. Lett.* vol. 8, pp. 1279-1282, 2009.

[13] B. K. Lau, "Multiple antenna terminals," in *MIMO: From Theory to Implementation*, C. Oestges, A. Sibille, and A. Zanella, Eds. San Diego: Academic Press, 2011, pp. 267-298.

[14] T. S. P. See, and Z. N. Chen, "An ultrawideband diversity antenna," *IEEE Trans. Antennas Propag.*, vol. 57, no. 6, pp. 1597–1605, Jun. 2009.

[15] M. Kahrizi, T. K. Sarkar, and Z. A. Maricevic, "Analysis of a wide radiating slot in the ground plane of a microstrip line," *IEEE Trans. Microwave Theory Tech.*, vol. 41, no. 1, pp. 29–37, Jan. 1993

[16] S. Zhang, S. N. Khan and S. He. "Reducing mutual coupling for an extremely closely-packed tunable dual-element PIFA array through a resonant slot antenna formed in-between," *IEEE Trans. Antenna Propag.* vol. 58, No. 8, pp. 2771-2776, Aug. 2010.

[17] R. Vaughan and J. B. Andersen, Eds., *Channels, Propagation and Antennas for Mobile Communications*. London, U.K.: IEE, 2003, pp. 569-576.

[18] R. Tian, B. K. Lau, and Z. Ying, "Multiplexing efficiency of MIMO antennas," *IEEE Antennas Wireless Propag. Lett.*, vol. 10, pp. 183-186, 2011.